

Gas jet structure influence on high harmonic generation

James Grant-Jacob,^{1,*} Benjamin Mills,¹ Thomas J Butcher,¹ Richard T Chapman,²
William S Brocklesby,¹ and Jeremy G Frey²

¹Optoelectronics Research Centre, University of Southampton, Southampton, SO17 1BJ, UK

²School of Chemistry, University of Southampton, Southampton, SO17 1BJ, UK

*jjg@orc.soton.ac.uk

Abstract: Gas jets used as sources for high harmonic generation (HHG) have a complex three-dimensional density and velocity profile. This paper describes how the profile influences the generation of extreme-UV light. As the position of the laser focus is varied along the jet flow axis, we show that the intensity of the output radiation varies by approximately three times, with the highest flux being observed when the laser is focused into the Mach disc. The work demonstrated here will aid in the optimization of HHG flux from gas jet sources. The flux increase is attributed to a density increase within the structure of the jet, which is confirmed by simultaneous imaging of atom and ion fluorescence from the jet.

©2011 Optical Society of America

OCIS codes: (100.0118) Imaging ultrafast phenomena; (190.4160) Multiharmonic generation.

References and links

1. R. Neutze, R. Wouts, D. van der Spoel, E. Weckert, and J. Hajdu, "Potential for biomolecular imaging with femtosecond X-ray pulses," *Nature* **406**(6797), 752–757 (2000).
2. R. Kienberger, E. Goulielmakis, M. Uiberacker, A. Baltuska, V. Yakovlev, F. Bammer, A. Scrinzi, Th. Westerwalbesloh, U. Kleineberg, U. Heinzmann, M. Drescher, and F. Krausz, "Atomic transient recorder," *Nature* **427**(6977), 817–821 (2004).
3. H. N. Chapman, A. Barty, M. J. Bogan, S. Boutet, M. Frank, S. P. Hau-Riege, S. Marchesini, B. W. Woods, S. Bajt, W. H. Benner, R. A. London, E. Plönjes, M. Kuhlmann, R. Treusch, S. Düsterer, T. Tschentscher, J. R. Schneider, E. Spiller, T. Möller, C. Bostedt, M. Hoener, D. A. Shapiro, K. O. Hodgson, D. van der Spoel, F. Burmeister, M. Bergh, C. Caleman, G. Huldt, M. M. Seibert, F. R. N. C. Maia, R. W. Lee, A. Szöke, N. Timneanu, and J. Hajdu, "Femtosecond diffractive imaging with a soft-X-ray free-electron laser," *Nat. Phys.* **2**(12), 839–843 (2006).
4. M. Lewenstein, Ph. Balcou, M. Yu. Ivanov, A. L'Huillier, and P. B. Corkum, "Theory of high-harmonic generation by low-frequency laser fields," *Phys. Rev. A* **49**(3), 2117–2132 (1994).
5. P. B. Corkum, "Plasma perspective on strong field multiphoton ionization," *Phys. Rev. Lett.* **71**(13), 1994–1997 (1993).
6. A. Rundquist, C. G. Durfee 3rd, Z. Chang, C. Herne, S. Backus, M. M. Murnane, and H. C. Kapteyn, "Phase-matched generation of coherent soft X-rays," *Science* **280**(5368), 1412–1415 (1998).
7. Ch. Spielmann, N. H. Burnett, S. Sartania, R. Koppitsch, M. Schnürer, C. Kan, M. Lenzner, P. Wobrauschek, and F. Krausz, "Generation of coherent X-rays in the water window using 5-femtosecond laser pulses," *Science* **278**(5338), 661–664 (1997).
8. P. M. Paul, E. S. Toma, P. Breger, G. Mullot, F. Augé, Ph. Balcou, H. G. Muller, and P. Agostini, "Observation of a train of attosecond pulses from high harmonic generation," *Science* **292**(5522), 1689–1692 (2001).
9. P. Salières, A. L'Huillier, and M. Lewenstein, "Coherence control of high-order harmonics," *Phys. Rev. Lett.* **74**(19), 3776–3779 (1995).
10. P. Balcou, P. Salières, A. L'Huillier, and M. Lewenstein, "Generalized phase-matching conditions for high harmonics: the role of field-gradient forces," *Phys. Rev. A* **55**(4), 3204–3210 (1997).
11. T. C. Adamson, Jr. and J. A. Nicholls, "On the structure of jets from highly underexpanded nozzles into still air," *J. Aerosp. Sci.* **26**, 16–24 (1959).
12. H. Ashkenas and F. S. Sherman, "Structure and utilization of supersonic free jets in low density wind tunnels," *Rarefied Gas Dyn.* **2**, 84–105 (1966).
13. H. Pauly, *Atom, Molecule, and Cluster Beams I* (Springer, 2000), Chap. 3.
14. C. G. Durfee III, A. R. Rundquist, S. Backus, C. Herne, M. M. Murnane, and H. C. Kapteyn, "Phase matching of high-order harmonics in hollow waveguides," *Phys. Rev. Lett.* **83**(11), 2187–2190 (1999).
15. K. L. Saenger, "Pulsed molecular beams: a lower limit on pulse duration for fully developed supersonic expansions," *J. Chem. Phys.* **75**(5), 2467–2469 (1981).

1. Introduction

Intense spatially coherent ultrashort soft-X-ray pulses are desired for biological and crystalline imaging at nm length scales [1–3]. Such radiation can be produced via high harmonic generation (HHG) [4,5], commonly achieved by focusing a high energy ultrashort laser pulse into a gas-filled capillary [6], gas cell [7] or gas jet [8]. The efficiency of generating harmonics is typically limited by a phase mismatch between the fundamental and generated harmonics, and the density of nonlinear material present – both of which are critically dependent on the gas source geometry.

In the case of a gas jet, as discussed in this paper, the phase matching is generally a balance between the Gouy phase, atomic phase, neutral gas and plasma dispersion. The strong dependence of the high harmonic intensity and generation efficiency on the positioning of the pump laser focus with respect to the gas jet along the direction of laser propagation (perpendicular to the jet flow axis) is well known [9,10]. We show that the efficiency of HHG is also strongly dependent on the position of the laser focus along the supersonic free jet flow axis arising from strong gas density variation within the jet structure. Side imaging of fluorescence from the jet during HHG illustrates the density variation within the jet and allows the accurate positioning of the laser focus to the highest density region of the jet, the Mach disc.

2. Experimental setup

In this experiment, a Ti:sapphire chirped pulse amplifier (CPA) system operating at 1 kHz repetition rate produced 1 mJ laser pulses with a duration of 40 fs. The beam was focused using a 50 cm lens to produce a spot size of 55 μm with a peak intensity of $4.8 \times 10^{14} \text{ W cm}^{-2}$ and a confocal parameter of $\sim 13 \text{ mm}$ in a vacuum chamber that has a 500 μm inner diameter tapered glass nozzle suspended inside. Ar gas was passed through the nozzle to create the free jet, and the relative height of jet to the laser focus could be altered. The position of the jet along the laser axis was accurately placed at the centre of the laser focus using side fluorescence imaging and was maintained in this position for all experiments to maintain similar phase matching conditions throughout. A 200 nm thick aluminium foil filter was used to separate the extreme-UV (XUV) and the fundamental laser so that harmonic emission between 20 and 60 nm could be observed using an XUV spectrometer with a microchannel plate (MCP) fluorescent screen and charged-coupled device (CCD) camera. Fluorescence emission from excited Ar species within the jet was imaged using a lens and CCD camera combination set at right angles to the laser and jet propagation axes. Particular emission lines were selected using a filter and were monitored simultaneously to XUV emission.

3. Results

Figure 1 shows a 420 nm fluorescence image of the jet with a backing pressure of 100 mbar. Here the axis of the jet flow is vertically downward and the laser is propagating from left to right, with the focus set at 1 mm below the nozzle aperture that is centred along the laser axis. This fluorescence image is produced by emission from highly excited Ar atoms and ions in Rydberg states created in the ionization and recombination process. The dominant emission in this instance is at 420 nm from excited Ar atoms, with a lifetime of $\sim 1 \mu\text{s}$. Excited atoms created within the laser beam volume will fluoresce after moving within the jet and so the fluorescence image is a convolution of the gas density, atom velocity, fluorescence lifetime and the rate constant for decay from excited ion to excited atom.

As gas leaves a jet nozzle at higher pressure than the background, it forms a cylindrical region of high pressure, slow moving gas known as the barrel shock that encompasses a region of fast moving, less dense over-expanded gas known as the zone of silence. Beyond the zone of silence is the Mach disc, where the gas slows down and recompresses, thus significantly increasing in density. This density increase can be clearly seen in Fig. 1 at a height of $\sim 2.7 \text{ mm}$ below the jet nozzle. The lifetime of the fluorescence is not long enough to see the full extent of the Mach disc in Fig. 1. From fluorescence images taken when focusing

the laser at other jet nozzle-laser distances, it is evident that the Mach disc extends further down the jet, peaking in density at ~ 3 mm. Beyond this is a further low pressure region formed by re-expansion [11]. The regions of stagnant gas either side of the jet show high fluorescence levels – however, this does not reflect the actual gas density in the stagnant region. Fluorescence is high in these regions and extends above 1 mm because the gas is not in the jet flow but diffusing within the vacuum chamber and moving much more slowly than gas in either the zone of silence or the Mach disc. The fluorescence signal is therefore not dispersed spatially as it is in these other regions of relatively fast moving gas. This is confirmed by observations of the fast emission from excited Ar ions at 488 nm.

The length scale of the structure is dependent on the jet nozzle diameter and the ratio of the backing pressure behind the jet to the background pressure in the region into which the jet is expanding [12]. The position of the Mach disc, x_M , is given by,

$$x_M = 0.67d \left(\frac{P_0}{P_b} \right)^{1/2} \quad (1)$$

where d is the nozzle diameter, P_0 is the backing pressure behind the jet and P_b is the pressure in the region into which the jet is expanding [12]. For the parameters used in this experiment, x_M is calculated using Eq. (1) to be ~ 3 mm at $P_0 = 100$ mbar, reducing to ~ 2 mm at $P_0 = 50$ mbar.

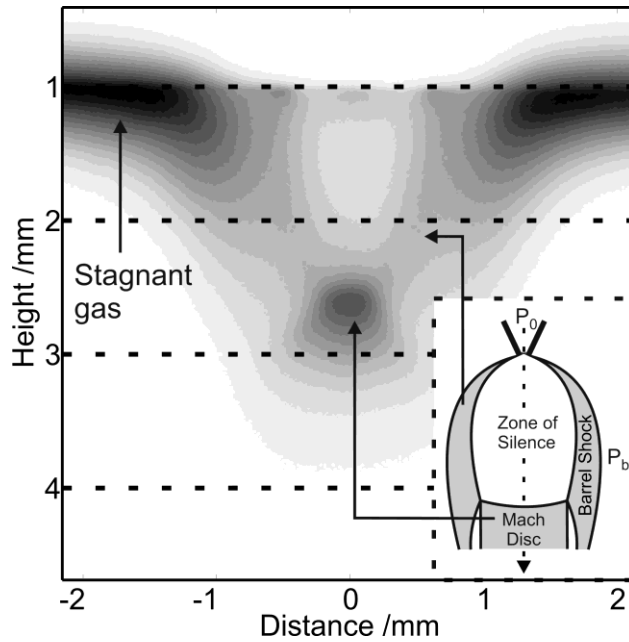


Fig. 1. Image of fluorescence at 420 nm formed predominantly from excited Ar atoms in the jet, viewed side on at 100 mbar jet backing pressure, with the four heights of probing marked. Inset - schematic of free jet expansion from a nozzle.

The four positions of the laser along the jet flow axis used in this experiment are shown by the dashed horizontal lines in Fig. 1. At a backing pressure of 100 mbar (corresponding to the image in Fig. 1), the focused laser passes through the zone of silence for jet nozzle-laser separations of 1 mm and 2 mm, which is a region where gas atoms have high velocities (Mach number $\gg 1$) and low density. When the nozzle is placed at a height of 3 mm above the laser axis, the laser focus passes through the Mach disc (which is a region of low velocities, Mach no. < 1) and at 4 mm, the laser is passing through the re-expansion region in which the particles have velocities of around Mach no. > 1 . The pressure in the Mach disc is estimated

from the fluorescence intensity to be 25 mbar, which is approximately twice the pressure in the barrel shock and expansion region, and over four times greater than that in the zone of silence.

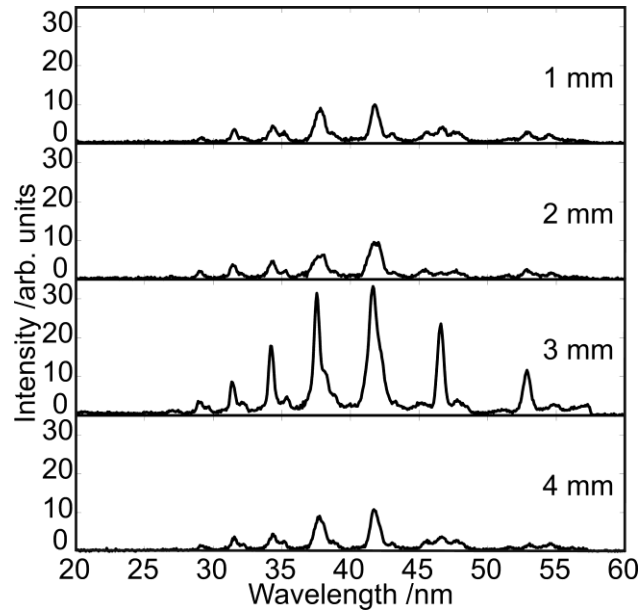


Fig. 2. Spectrum of XUV emission at 100 mbar jet backing pressure for jet nozzle-laser separations 1, 2, 3 and 4 mm, showing increase in yield at 3 mm across the XUV spectrum.

Figure 2 shows the different XUV spectra obtained with a backing pressure of 100 mbar when the laser focus is translated down the axis of the jet to the positions shown in Fig. 1. The generated XUV flux varies significantly, with highest intensities being achieved when the laser is focused 3 mm below the nozzle exit, at the position of the Mach disc. From these spectra, it is apparent that as the laser focus is brought into the Mach disc, the intensity of all the harmonics shows a significant increase, with the greatest difference being for the 17th harmonic (~ 46 nm) where a tenfold increase in flux is obtained.

The highest overall intensity attained for all laser positions is for the 19th harmonic (~ 41 nm). The yield for this harmonic is plotted in Fig. 3 as a function of pressure for all four jet nozzle-laser separations probed by the laser. For positions of 1 mm, 2 mm and 4 mm, away from the Mach disc, the variation of output with pressure is quadratic. A quadratic fit to the variation is shown on the figure for all four heights – the same fit parameters are shown on each graph. At heights of 2 mm and 3 mm there are deviations from this quadratic behaviour at pressures of 50 mbar and ~ 100 mbar respectively. In particular, the large increase in harmonic output signal at a jet nozzle-laser separation of 3 mm at pressures around 100 mbar is clearly seen. This corresponds to the laser passing through the Mach disc formed at a backing pressure of 100 mbar, as illustrated by Fig. 1.

Both theoretical calculations and side fluorescence images indicate that the Mach disc moves towards the jet nozzle as the backing pressure is lowered. At 50 mbar, the Mach disc is 2 mm from the nozzle, and at 100 mbar, the Mach disc is 3 mm from the nozzle. Because of the square-root dependence of position on pressure, a Mach disc position of 4 mm is never reached in our experiment. The background pressures are such that at a backing pressure low enough to give a Mach disc position of 1 mm, supersonic flow is not established and the jet is mostly effusive, with no distinct Mach disc [13].

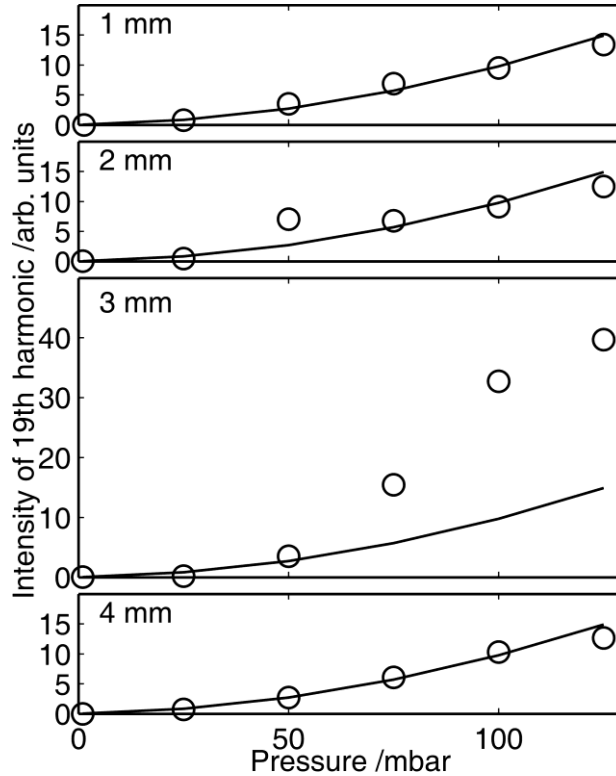


Fig. 3. Intensity of the 19th harmonic as a function of pressure at different jet nozzle-laser separations, showing deviation from quadratic variation at heights of 2 mm (at 50 mbar) and 3 mm (around 100 mbar).

The intensity of harmonic output of the q th harmonic can be written generally as [14]:

$$|E_q|^2 \approx N^2 |\chi_{eff}^{(q)} E_0|^2 \left(\frac{1 + e^{-2\alpha L} - 2e^{-\alpha L} \cos \Delta k L}{\alpha^2 + \Delta k^2} \right) \quad (2)$$

where N is the number density of atoms, $\chi_{eff}^{(q)}$ is the effective nonlinear polarization, E_0 is the input field, s is the effective order of the nonlinearity (~ 5), α is the absorption coefficient and Δk is the wavevector mismatch. The final bracketed term describes the contribution of phase matching to the final harmonic output intensity in the presence of absorption and reduces to the familiar $\text{sinc}^2(\Delta k L/2)$ term if α is small. Contributions to the spatially-varying wavevector mismatch Δk arise from the Gouy shift, the atomic phase contribution due to the delay in emission depending on electron trajectory, the refractive indices of the gas at pump and harmonic wavelength, and the refractive index of the plasma created by ionization. In this experiment, the peak intensity of the laser will cause significant ionization of the gas, both reducing the effective number density and increasing the plasma contribution to the refractive index at the centre of the focus.

Evaluation of Eq. (2) through the focus shows that when the jet is placed axially at the centre of the laser focus, almost all the generation is from the short trajectory atomic phase component. Although harmonics generated from the long trajectory atomic phase component generally have long coherence lengths at the laser focus [10], in this work, generation from the centre of the beam does not contribute to the final output at the harmonic wavelengths due to the high level of ionization. All of the generated harmonic intensity comes from radii towards the edge of the beam, in a region extending from where ionization drops off, to the region where the laser intensity drops below cut-off. For the 19th harmonic, this region extends from 25 – 35 μm from the beam centre. In this region, the coherence length is $\geq 1\text{mm}$,

even for the highest gas densities used in this experiment. Hence for a 500 μm jet width, the buildup of harmonic in this region is not limited by the phase matching term in Eq. (2). This is confirmed by the overall quadratic dependence of harmonic output with pressure in regions where the jet's spatial structure does not change rapidly with pressure – either close to the nozzle or beyond the Mach disc.

The actual gas density at the heights at which XUV is generated depends directly on the spatial structure of the jet. Once the jet is established, at a distance of typically five times the nozzle diameter, the flow of gas is roughly cylindrical and so density is dependent on the gas velocity. When the laser intersects the zone of silence, there are contributions to generation from the dense but thin barrel shock region and from the less dense zone of silence region, but the total number of gas atoms contributing to HHG is small. When the laser intersects the Mach disc, the density is increased across the whole jet, and the number of atoms contributing the HHG increases significantly, as demonstrated by the increase in high harmonic signal shown in Fig. 3. The background quadratic increase in signal level with pressure is seen to be approximately the same at 1 mm, 2 mm, and 4 mm levels. This is a consequence of the similar gas velocities and densities within the cylindrical jet in these regions.

Such behavior should also be observed with pulsed gas jets under the same experimental conditions, as long as the laser pulse interacts with the jet at a time after the gas behind the nozzle has accelerated, expanded and then equilibrated, since by this time, the jet structure will be the same as that of a continuous gas jet. As an example, for a 500 μm Ar jet at 267 mbar backing pressure, establishment of the jet structure takes $\sim 10 \mu\text{s}$ [15].

4. Conclusion

In summary, we have demonstrated the variation in high harmonic output from an Ar gas jet arising from the complex spatial structure of the jet itself, and by comparison with fluorescence imaging and analysis of the phase matching in this experimental geometry, we have shown that the increase in density at the Mach disc produces a significant increase in high harmonic signal. As a result, not only is the relative position of a gas jet along the laser axis critical to HHG efficiency, but so is the position of the laser focus along the jet flow axis.

Acknowledgments

This work was supported by the Research Councils U.K. through the Basic Technology Programme (Contract No. R87307). U.K. Engineering and Physical Sciences Research Council (EPSRC) DTA studentships supported JG-J, TJB and RTC.